Chapter 17

Ultrasound of the Kidneys and Adrenal glands

17. Ultrasound of the Kidneys and Adrenal glands

Seung Hyup Kim, Vito Cantisani, Michele Bertolotto

17.1. Ultrasound of the Kidneys

17.1.1. Patient positions and respiration, and machine setting

To obtain clear US images of the kidneys, we need to have a proper transducer position, proper patient posture, and proper patient respiration. In supine position with slight elevation of the side of the examination or lateral decubitus position is usually enough, but if we have a difficulty with these postures we may ask the patient to have a prone position for better visualization of the kidneys (→ Chapter 10).

17.1.2. Normal grey-scale ultrasound findings

The length of the normal kidneys usually ranges between 9cm and 12cm. We may measure the approximate volume of the kidney by prolate ellipse formula (length x width x thickness x π/6). The volume of the normal adult kidneys is usually between 100mL and 200mL. Parenchymal thickness and cortical thickness may be measured as well. In adults, normal parenchymal thickness is usually between 15mm and 20mm while normal cortical thickness is usually between 7mm and 10mm (→ Chapter 10). The echogenicity of the normal renal cortex is slightly lower than that of the liver or spleen.

17.1.3. Normal Doppler ultrasound findings

The kidney is a hypervascular organ and can be evaluated with Doppler ultrasound. General status of renal blood flow can easily be assessed with color Doppler US (CDUS). Power Doppler US (PDUS) is more sensitive than CDUS in demonstrating smaller vessels with less flow. Various newer Doppler techniques have been developed to improve sensitivity to show flow in the periphery of the renal parenchyma. Spectral Doppler US (SDUS) is important in evaluation of the kidneys and is usually performed at the interlobar artery level. Doppler spectral analysis provides important information regarding hemodynamic status of the kidney and peripheral renal vascular resistance.

A correct measurement of renal resistive index (RI) needs a standardized study protocol. First of all, a correct visualization of the kidney is obtained, with a precise regulation of focus and gain. Then, the color box is regulated, and Doppler parameters optimized to obtain an optimal depiction of the vessels undergoing interrogation. The equipment is set with the highest gains below the noise threshold, lowest possible filters, and a low pulse repetition frequency (PRF). After these settings, the sample volume is placed in the vessel and Doppler spectrum obtained. To obtain a correct sampling, a careful setting of Doppler parameters (Doppler frequency, PRF, gain, wall filter) is a crucial step. The renal RI is calculated through the measure of the peak systolic velocity (PSV) and the end diastolic velocity (EDV) according to the formula: (PSV–EDV)/PSV. Multiple Doppler measurements should be obtained in different areas of the kidney (i.e., upper pole, midportion, and lower pole). It is important to interrogate the renal vessels at the same level, since PSV and RI reduce when moving from the segmental, to the interlobar/arcuate, to the interlobular arteries. Measurement at the level of interlobar/arcuate arteries is preferred.

Normal RI is usually around 0.6, and 0.7 is regarded as the upper normal limit of RI. Renal Doppler RI is lowest in young adults and is slightly higher in young children and old aged adults. RI changes are often non-specific. They cannot be considered alone a marker of renal damage, nor a prognostic indicator of renal damage progression. When considered in the proper clinical setting, however, measurement of renal RI may provide useful information for a more accurate assessment of the nephropatic patient. In particular, RI provides information about the link between micro- and macro-circulation of the kidney, and is correlated with biopsy parameters such as vascular and tubulointerstitial lesions.

The term renal RI is sometimes used as a synonym of vascular resistance. This is a misleading simplification, as a variety of systemic and renal parameters affect RI values. Among them, blood pressure, cardiac function, vascular compliance, and renal capillary wedge pressure are the most important hemodynamic factors to be considered.

The Renal RI can be useful to make a differential diagnosis between prerenal and renal causes of acute kidney injury (AKI). Prerenal AKI is characterized by reduction in renal perfusion, generally associated with normal RI. Renal causes for AKI are more frequently characterized by increased RI.

In chronic kidney disease, increased RI (≥0.70) is an independent risk factor for the progression of renal failure. A significant correlation exists between RI values ≥0.70 or higher in chronic nephropathies and parenchymal irreversible damage. In patients with renal artery stenosis, RI values >0.80 are predictive of poor improvement of renal function after revascularization. In patients with moderate renal dysfunction, a renal RI values ≥0.79 is a predictor for the annual decline in estimated glomerular filtration rate, and a negative prognostic indicator for cardiovascular events.

Remember

- A correct measurement of renal resistive index (RI) needs a standardized study protocol
- Normal renal RI is usually around 0.6
- In acute kidney injury, renal RI can be used to differentiate between prerenal (normal RI) and renal (increased RI) causes
- In chronic kidney disease, increased RI (≥0.70) is an independent risk factor for the progression of renal failure

17.1.4. Normal variations

17.1.4.1. Prominent column of Bertin

The column of Bertin is a thickened aggregate of the cortical tissue instead of the usual thin cortical septum that separates two pyramids. It is the most common cause of renal pseudotumors at US and may mimic renal tumors. The junction of the upper and middle thirds of the kidney is the most common site of prominent column. CDUS or PDUS may demonstrate blood vessels passing through the lesion, unlikely the true parenchymal tumor in which the vessels are usually stretched and displaced in the periphery of the mass. In case of doubt, when the normal branching of the renal parenchymal vessels is not depicted within the pseudotumor, CEUS is able to show a cortical and a medullary portion, which enhance at different times.

17.1.4.2. Junctional parenchymal defect

Frequently triangular echogenic areas are seen in polar areas of the kidney. These defects in the parenchyma result from extension of the renal sinus fat due to incomplete fusion of two embryogenic renal parenchymatous masses.

This normal variation can be differentiated from pathologic conditions such as parenchymal scarring or angiomyolipoma by its characteristic location and continuity with the renal sinus (Fig 17.1) (→ Chapter 10).

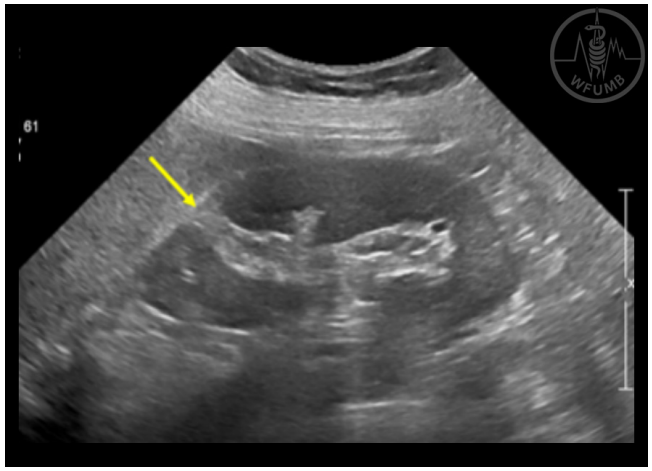

View enlarged image

Fig 17.1a
Junctional parenchymal defect in a 61-year-old woman. Echogenic cortical defect (arrow) in the upper polar area of the kidney which is continuous with the renal sinus echo

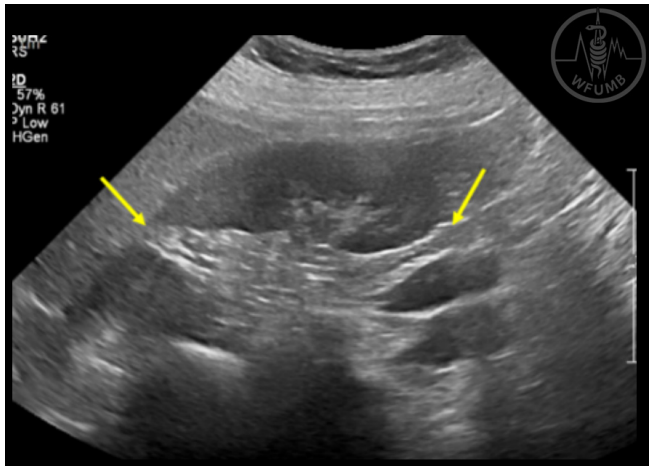

View enlarged image

Fig 17.1b
Junctional parenchymal defects in a 61-year-old woman. Echogenic cortical defects (arrows) in the upper and lower polar areas of the kidney which is continuous with the renal sinus echo

17.1.5. Renal parenchymal diseases

Renal parenchymal disease may be divided into glomerular and tubulointerstitial disease. In early phase of various renal parenchymal disease, kidney may be enlarged and edematous but it becomes smaller as the disease becomes chronic.

Usually there are changes in renal parenchymal echoes in renal parenchymal disease. Renal cortical echogenicity is increased and CMD becomes indistinct (Fig 17.2). Infrequently CMD may be accentuated (Fig 17.3). Doppler RI is usually preserved in glomerular diseases but is elevated in tubulointerstitial diseases.

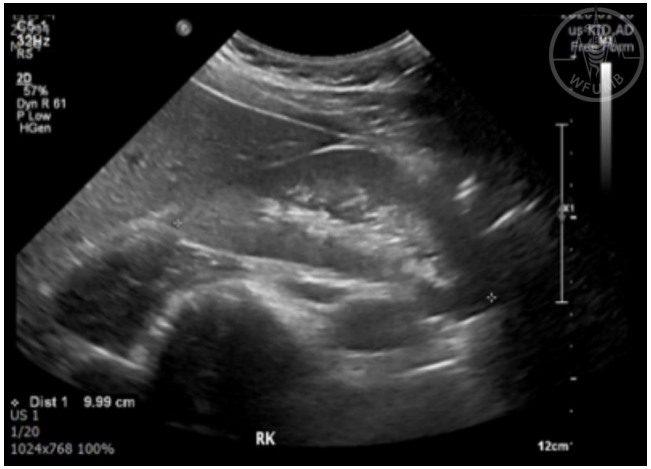

View enlarged image

Fig 17.2a
35-year-old man with IgA nephropathy. Grey-scale US of the right kidney shows diffusely increased echogenicity of the renal parenchyma and obliterated CMD

View enlarged image

Fig 17.2b
35-year-old man with IgA nephropathy. Grey-scale US of the left kidney shows diffusely increased echogenicity of the renal parenchyma and obliterated CMD

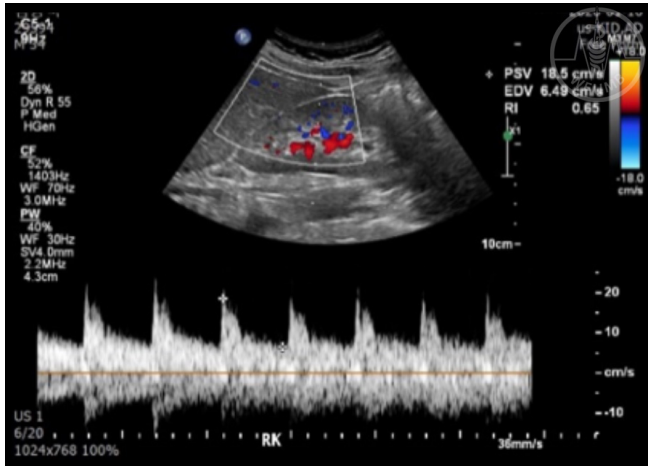

View enlarged image

Fig 17.2c
35-year-old man with IgA nephropathy. SDUS image of the right kidney shows normal Doppler spectral patterns and normal RI (right 0.65; left 0.63 - not shown)

View enlarged image

Fig 17.3a
Tubulointerstitial nephritis in a 62-year-old man. Grey-scale US image of the right kidney shows diffusely increased echogenicity of the renal cortex and slightly accentuated CMD

View enlarged image

Fig 17.3b
Tubulointerstitial nephritis in a 62-year-old man. Grey-scale US image of the left kidney shows diffusely increased echogenicity of the renal cortex and slightly accentuated CMD

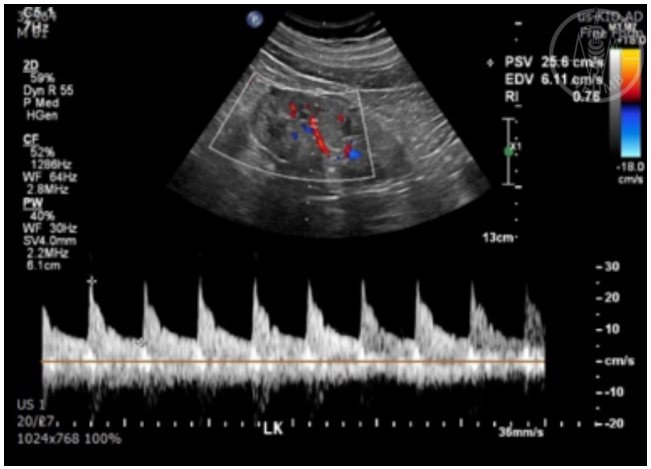

View enlarged image

Fig 17.3c
Tubulointerstitial nephritis in a 62-year-old man.SDUS image of the right kidney shows elevated Doppler resistive index (right 0.76; left 0.78 - not shown)

In most of renal parenchymal diseases, kidneys become smaller as the disease becomes chronic. Renal parenchymal volume is decreased and renal parenchyma and renal cortex become thin. In chronic kidney diseases, renal blood flow is usually diminished.

In patients with diabetes kidneys are enlarged in early stage of nephropathy due to hyper-filtration (Fig 17.4). As diabetic nephropathy aggravates, kidney becomes smaller. Even in case of advanced diabetic nephropathy, kidney may appear quite normal at grey-scale US images, but Doppler US is helpful in showing elevated Doppler RI.

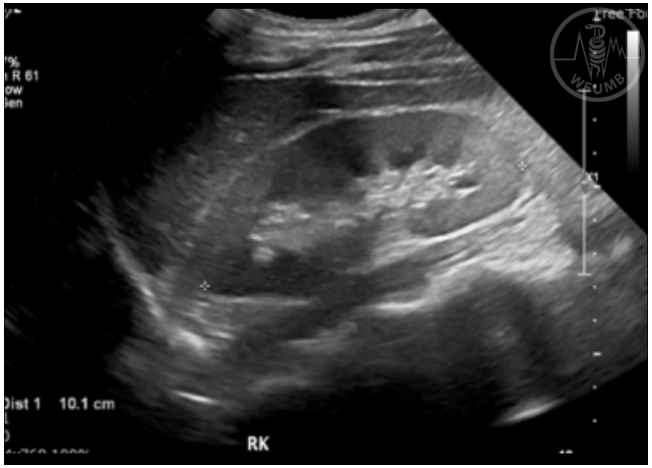

View enlarged image

Fig 17.4a
47-year-old man with diabetic nephropathy. Grey-scale US image of the right kidney shows normal size and shape of the kidney. Note renal parenchyma is slightly thick and CMD is slightly poor

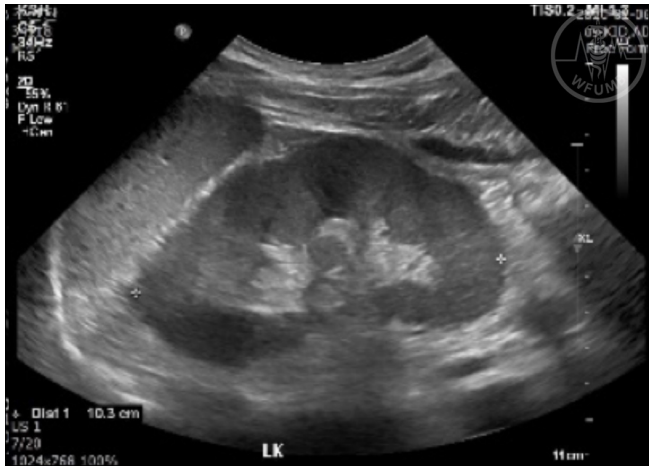

View enlarged image

Fig 17.4b
47-year-old man with diabetic nephropathy. Grey-scale US image of the kidney shows normal size and shape of the kidney. Note renal parenchyma is slightly thick and CMD is slightly poor

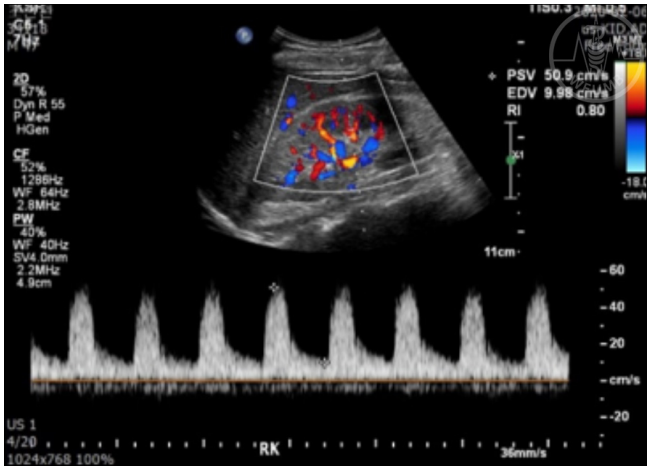

View enlarged image

Fig 17.4c
47-year-old man with diabetic nephropathy. SDUS shows high resistance pattern of the Doppler spectra and elevated RI (right 0.80; left 0.77 - not shown)

17.1.6. Renal masses

When renal masses are found, the first step to characterize them is a differentiation between cystic and solid ones (Fig 17.5). US has an excellent ability to differentiate between cystic and solid masses.

US criteria of a simple cyst are round shape, thin wall, no internal echoes, and posterior enhancement (Fig 17.6). If a cyst-like mass does not display all those criteria of a simple cyst, it should be evaluated carefully. Often the masses are indeterminate and have mixed cystic and solid appearances. In characterizing a mixed cystic and solid mass, an important finding is evidence of blood flow in solid-looking areas, which may be evaluated with CDUS or PDUS. Contrast-enhanced US (CEUS) is a sensitive technique to determine scanty amount of blood flow in the tissue. It can be used to characterize hypovascular solid lesions, and to detect vascular components in cystic lesions, allowing differentiation among cystic masses with different risk of malignancy, according to the Bosniak criteria.

When a mass appears solid, further characterization and differentiation among various solid renal tumors is needed. Angiomyolipoma typically appears homogeneously hyperechoic (Fig 17.5) but there are various atypical appearances. Most important, renal cell carcinomas (RCCs) have various echogenicity and, when small, can be markedly hyperechoic, resembling angiomyolipomas.

In fact, characterization of angiomylipomas cannot be safely obtained at US, but requires identification of intralesional fat tissue components at CT or at MRI. RCCs often have different imaging characteristics according to their subtypes (Fig 17.6). Clear cell RCC, which is the most common subtype, usually has heterogeneous hypervascular appearance while the second most common papillary RCCs are usually homogeneous and hypovascular. US alone is not enough to characterize renal masses other than simple cysts, and usually CT and/or MRI or CEUS are necessary for further evaluation.

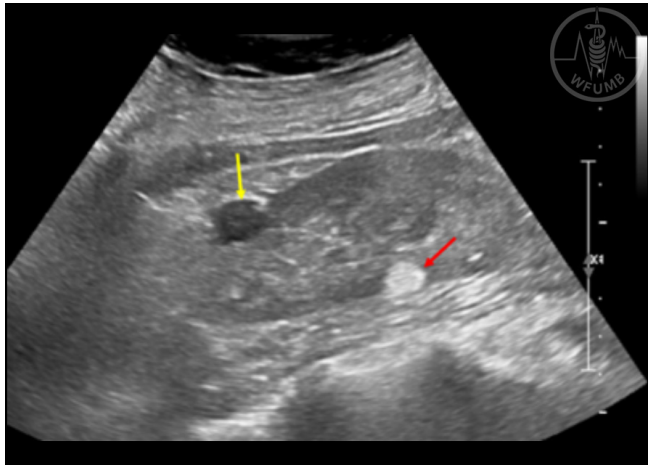

View enlarged image

Fig 17.5
Small cortical cyst and angiomyolipoma in the same kidney in a 62-year-old woman. Longitudinal US image of the right kidney shows a small anechoic renal cyst (yellow arrow) in the anterior aspect and a hyperechoic angiomyolipoma (red arrow) in the posterior aspect of the right kidney

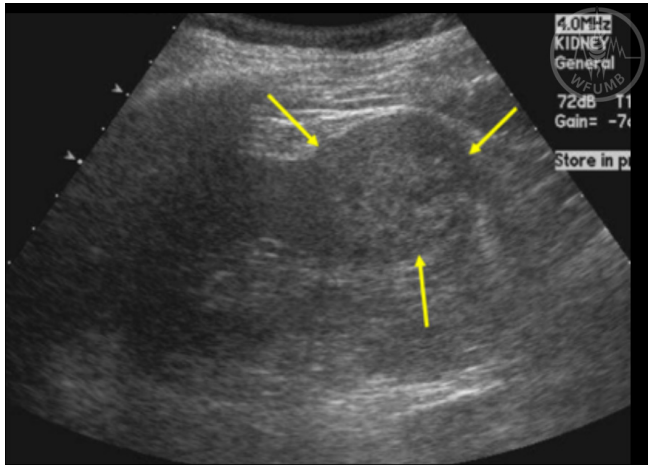

View enlarged image

Fig 17.6a
Two most common subtypes of renal cell carcinomas, clear cell type and papillary type. Clear cell RCC in a 49-year-old man showing heterogeneous appearance on B-mode US (arrows)

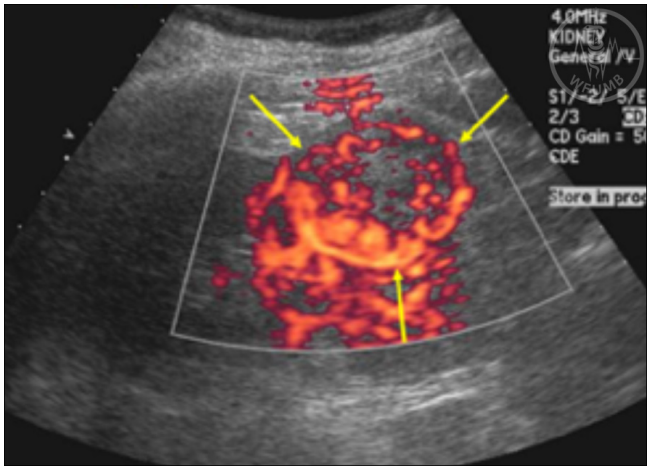

View enlarged image

Fig 17.6b
Two most common subtypes of renal cell carcinomas, clear cell type and papillary type. Clear cell RCC in a 49-year-old man showing and hypervascular appearance in CDUS (arrows)

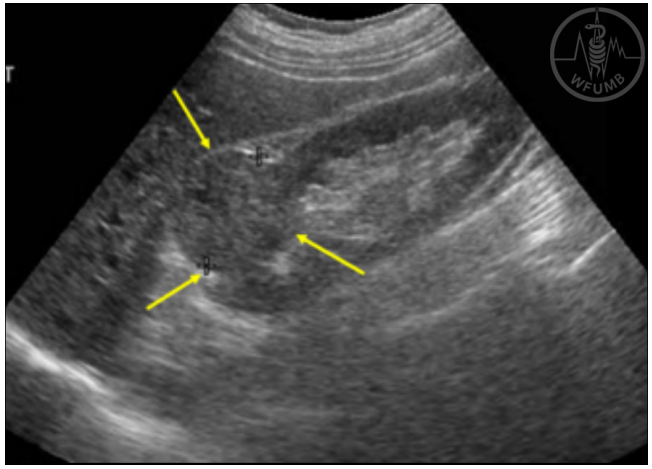

View enlarged image

Fig 17.6c
Two most common subtypes of renal cell carcinomas, clear cell type and papillary type. Papillary renal cell carcinoma in an 83-year-old man showing homogenous appearance in B-mode UD (arrows)

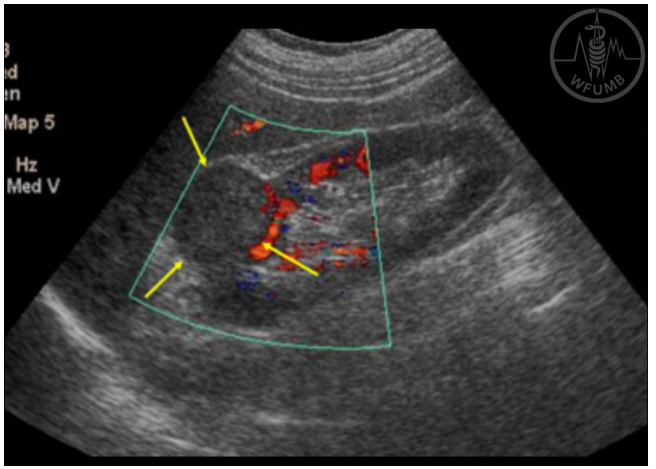

View enlarged image

Fig 17.6d
Two most common subtypes of renal cell carcinomas, clear cell type and papillary type. Papillary renal cell carcinoma in an 83-year-old man showing hypovascular appearance in CDUS (arrows)

17.1.7. Hydronephrosis

Dilatation of renal pelvis and calyces, i.e., hydronephrosis, can be detected easily with US, which has a major role for detection and identification of the cause of obstruction (Fig 17.7). Transient hydronephrosis may be caused by filled urinary bladder. Non-obstructive dilatation of the pelvicalyceal system, such as in reflux, should be differentiated by obstructive hydronephrosis, as well as mimicking situations such as parapelvic cysts and prominent renal hilar vessels that may mimic dilated renal pelvis or calyces (Fig 17.8). In hydronephrosis, however, the dilated calyces merge into a dilated renal pelvis, while parapelvic cysts do not merge into the renal pelvis. Hydronephrosis produced by ureteral obstruction both the renal pelvis and the ureter are dilated, while in ureteropelvic junction obstruction the ureter is not dilated.

There have been reports showing the value of Doppler spectral analysis in differentiating obstructive and non-obstructive hydronephrosis. However, it is not practical to use Doppler RI for this purpose. It is known that Doppler RI is elevated in acute and severe obstruction.

View enlarged image

Fig 17.7a
Hydronephrosis due to ureteral obstruction by uterine cervical carcinoma in a 69-year-old woman. US of the right kidney in longitudinal plane shows dilated renal pelvic and branching calyces of the right kidney

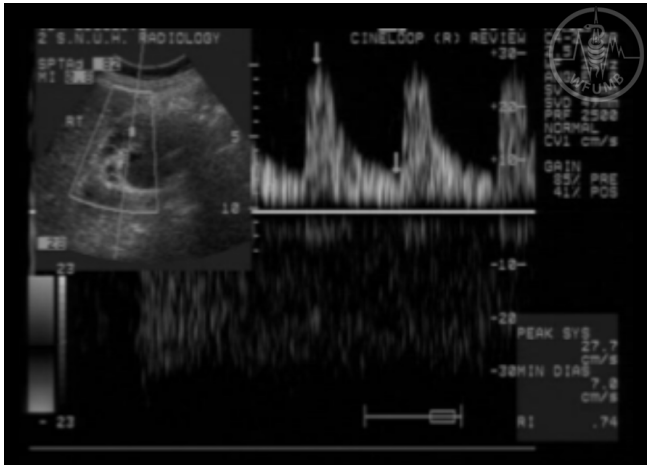

View enlarged image

Fig 17.7b
Hydronephrosis due to ureteral obstruction by uterine cervical carcinoma in a 69-year-old woman. Doppler US of the intrarenal artery of the right kidney shows slightly elevated Doppler RI of 0.74

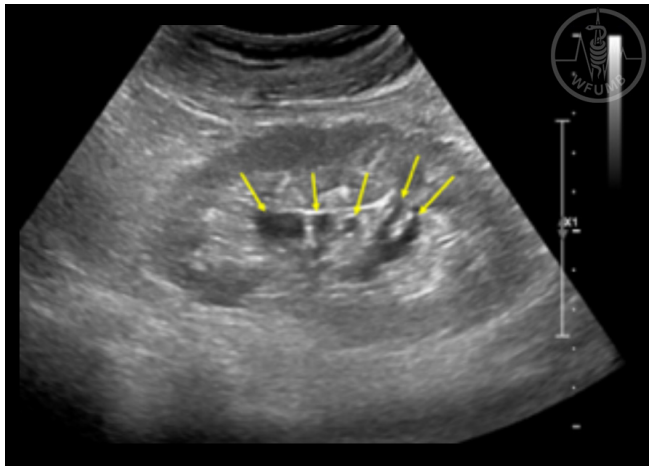

View enlarged image

Fig 17.8a
Parapelvic cysts mimicking hydronephrosis in an 81-year-old man. Grey-scale US image of the left kidney in longitudinal plane shows multiple cystic lesions of variable shape (arrows) in the central renal sinus area. Note that those cystic lesions are not connected to each other

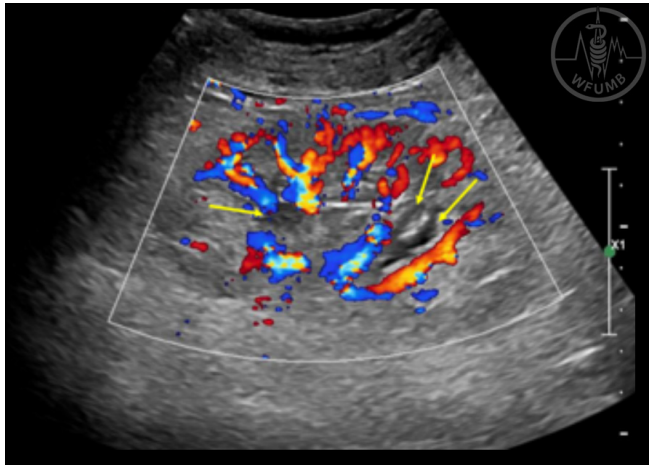

View enlarged image

Fig 17.8b
Parapelvic cysts mimicking hydronephrosis in an 81-year-old man. CDUS image shows that these lesions (arrows) are not vessels

Ultrasound classification of hydronephrosis:

- Grade I - only dilatation of the renal pelvis
- Grade II - dilatation of the pelvis and of the calyces without renal parenchymal atrophy
- Grade III - dilatation increases and initial signs of parenchymal atrophy are present
- Grade IV - marked dilatation of the renal pelvis and calyces with marked renal parenchymal atrophy

17.1.8. Renal calculi and nephrocalcinosis

US is helpful in detecting stones in the renal pelvicalyceal system and urinary bladder. It is not easy, however, to demonstrate ureter stones with US unless it is accompanied by ureteral dilatation. Sometimes, detection of urinary stones with US may be problematic when they are obscured by beam-attenuating tissues such as renal sinus fat, bowel gas, or when their posterior shadowing is weak. Twinkling artifacts at CDUS from urinary stones occur frequently and may be helpful in the diagnosis, especially in the cases of urinary stones with indistinct echo difference and indistinct posterior acoustic shadowing (Fig 17.9).

Nephrocalcinosis represents calcifications in the renal parenchyma. It can be divided into cortical nephrocalcinosis and medullary nephrocalcinosis with respect to the locations of calcification. The most common cause of cortical nephrocalinosis is renal cortical necrosis and those of medullary nephrocalcinosis are hyperparathyroidism, renal tubular acidosis, and medullary sponge kidney.

In cortical nephrocalcinosis, US images show increased peripheral cortical echogenicity and generate acoustic shadowing. On US, medullary nephrocalcinosis appears as increased echogenicity of the renal medulla resulting in reversal of the normal corticomedullary echogenicity which is called hyperechoic renal medulla (Fig 17.10). Small echogenic foci at the tips of medullary pyramids represent foci as precursors of renal calculi.

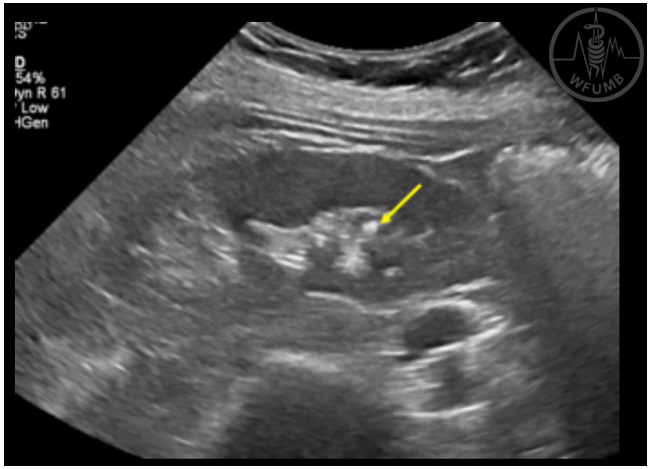

View enlarged image

Fig 17.9a
Twinkling artifact in a 61-year-old woman with a small stone in a tip of the calyx. Grey-scale US image of the right kidney shows a small echogenic lesion (arrow) in the lower pole area. The lesion does not have definite posterior sonic shadowing

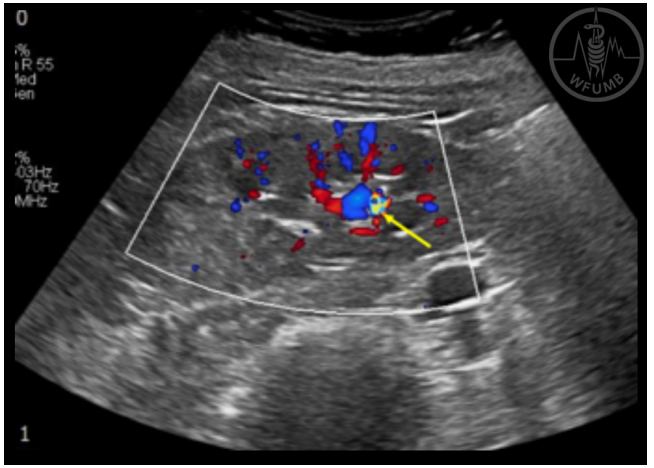

View enlarged image

Fig 17.9b
Twinkling artifact in a 61-year-old woman with a small stone in a tip of the calyx.
CDUS shows strong twinkling artifact (arrows) that is helpful in detecting small stones

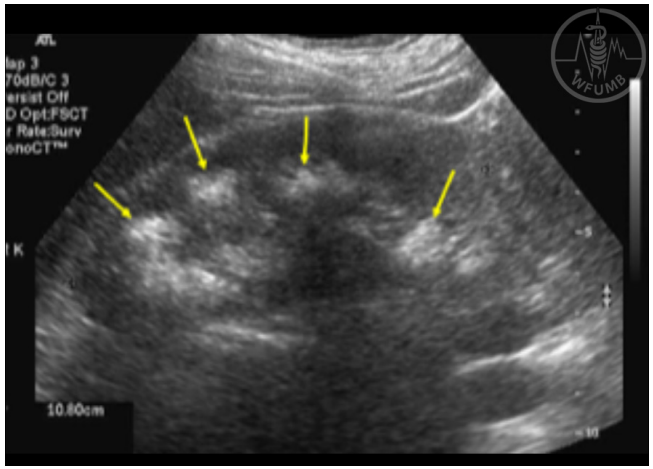

View enlarged image

Fig 17.10a
Medullary nephrocalcinosis due to renal tubular acidosis in a 45-year-old woman. Grey-scale US image of the right kidney in longitudinal plane shows hyperechoic renal medulla (arrows) due to medullary nephrocalcinosis

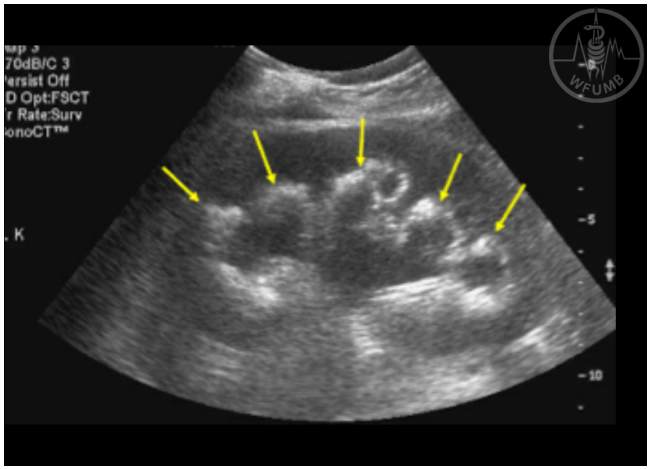

View enlarged image

Fig 17.10b
Medullary nephrocalcinosis due to renal tubular acidosis in a 45-year-old woman. Grey-scale US image the left kidneys in longitudinal plane shows hyperechoic renal medulla (arrows) due to medullary nephrocalcinosis. Mild hydronephrosis of the left kidney due to ureter stone

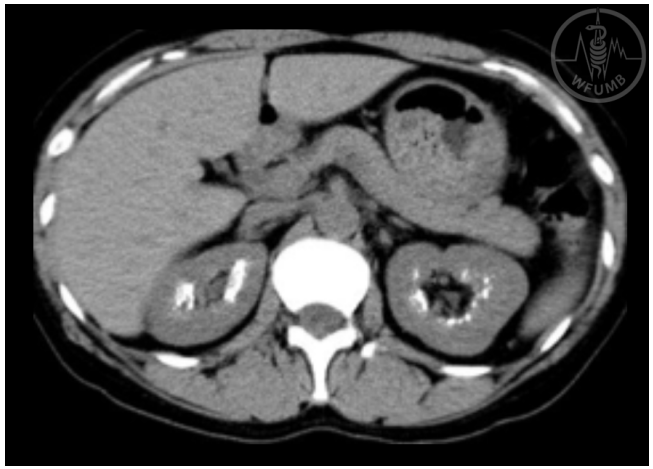

View enlarged image

Fig 17.10c
Medullary nephrocalcinosis due to renal tubular acidosis in a 45-year-old woman. Non-enhanced CT of the kidney shows fine calcification sin the renal medullary regions, both kidneys

17.1.9. Renal vascular disease

US, especially Doppler US, plays an important role in the evaluation of various renal vascular diseases such as renal artery stenosis or nutcracker syndrome.

17.1.9.1. Renal artery stenosis

Renal artery stenosis (RAS) is the most common cause of renal vascular hypertension and common underlying diseases are atherosclerosis, fibromuscular dysplasia, and Takayasu arteritis. Various imaging modalities can be used in the diagnosis of RAS but Doppler US is a useful initial imaging study (Fig 17.11).

There are two techniques to detect RAS using Doppler US. One is to evaluate the site of stenosis at main renal artery by detecting high peak systolic velocity, spectral broadening, and high ratio of peak systolic velocities of renal artery and aorta. Evaluation of whole length of main renal arteries may be difficult due to overlying bowel gas. Also, this technique alone may miss a stenosis at segmental artery level.
The other way of Doppler US to detect RAS is to evaluate Doppler spectral patterns of intrarenal arteries. The criteria that can be used are prolonged acceleration time which is the time interval between the start of the systole and peak systole, diminished acceleration index that is the slope of the systolic rise, and the loss of early systolic compliance peak.

Instead of these objective criteria, we may use observational changes of Doppler spectral pattern namely pulsus tardus and parvus which means slow-rising and weak pulse. Advantages of this technique, as compared to the technique focusing on the site of stenosis in the main renal artery, are that it is easier and has reasonably high sensitivity and specificity. Stenosis at segmental arterial level can be detected with this intrarenal Doppler technique.

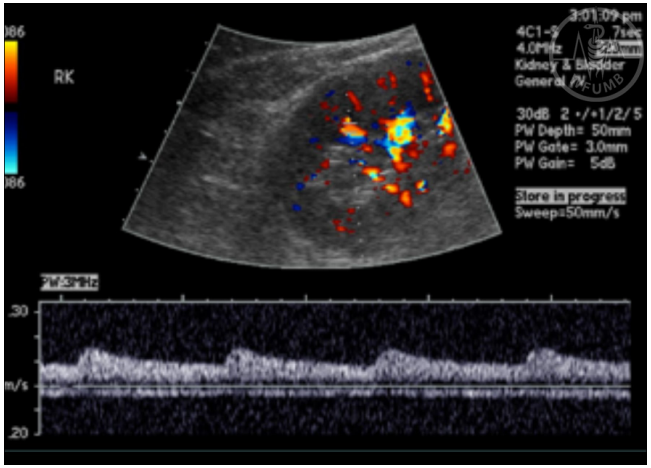

View enlarged image

Fig 17.11a
Unilateral renal artery stenosis in a 70-year-old hypertensive man. SDUS of the right kidney shows slow and weak pulse (pulsus tardus and parvus) pattern

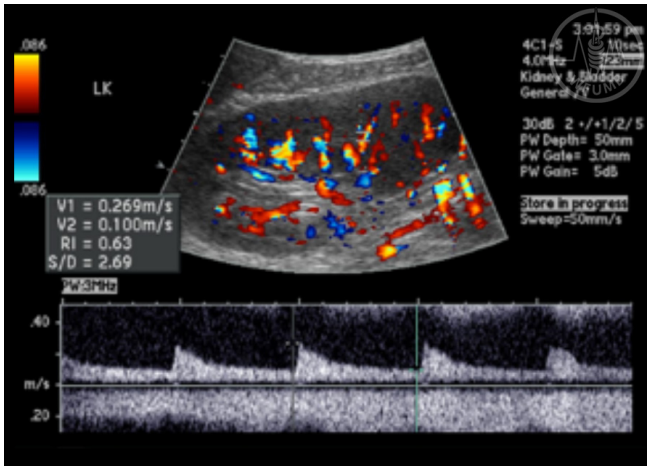

View enlarged image

Fig 17.11b
Unilateral renal artery stenosis in a 70-year-old hypertensive man. SDUS of the left kidney shows normal Doppler spectral pattern with sharp systolic peak

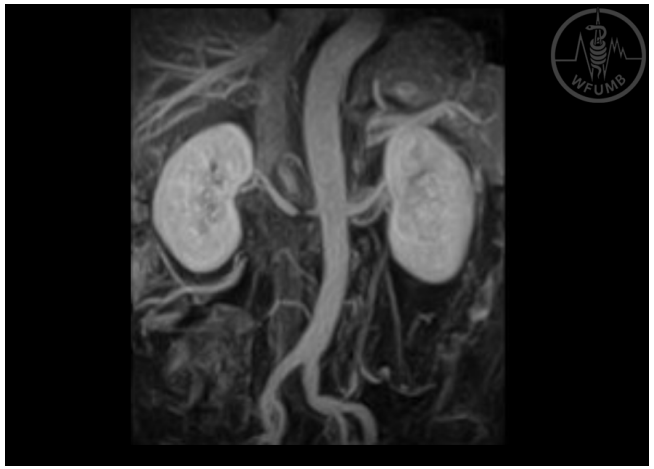

View enlarged image

Fig 17.11c
Unilateral renal artery stenosis in a 70-year-old hypertensive man. MR angiography shows a stenotic lesion (arrow) in the right renal artery

17.1.9.2. Nutcracker syndrome

Nutcracker syndrome is a disorder that occurs when the left renal vein (LRV) is compressed between the abdominal aorta and the superior mesenteric artery. Normally LRV is slightly compressed in this portion but when it is severely compressed, it causes proximal venous hypertension and the patients may show hematuria, proteinuria, and/or left flank pain. This syndrome is probably not as rare as it is known to be. Nutcracker phenomenon is a term describing the phenomenon while nutcracker syndrome is a term describing a condition when a patient with this phenomenon has related signs or symptoms such as hematuria, proteinuria, or left flank pain.

Normally peak flow velocity of LRV at aortomesenteric portion is around 40 to 50 cm/sec. A simple and practical Doppler criterion to suspect nutcracker phenomenon is 100cm/sec peak flow velocity in this location (Fig 17.12). There are variations of the velocity values according to the respiration and posture of the patients. Typically, this compression phenomenon occurs between abdominal aorta and superior mesenteric artery but there are other variations. LRV may be compressed by anteriorly-arising right renal artery and also LRV may be stretched over the abdominal aorta. Nutcracker phenomenon may occur in patients with venous anomalies such as retroaortic LRV, left-sided or double inferior vena cava.

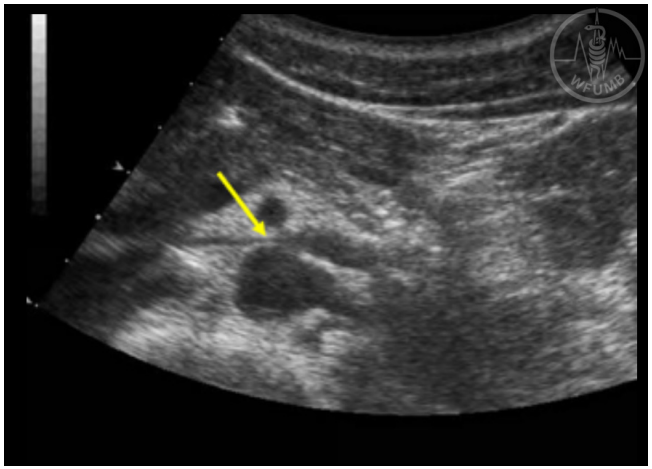

View enlarged image

Fig 17.12a
19-year-old man with gross hematuria caused by nutcracker syndrome. Grey-scale US image in transverse plane shows left renal vein (LRV) compressed between the aorta and superior mesenteric artery (SMA) (arrow)

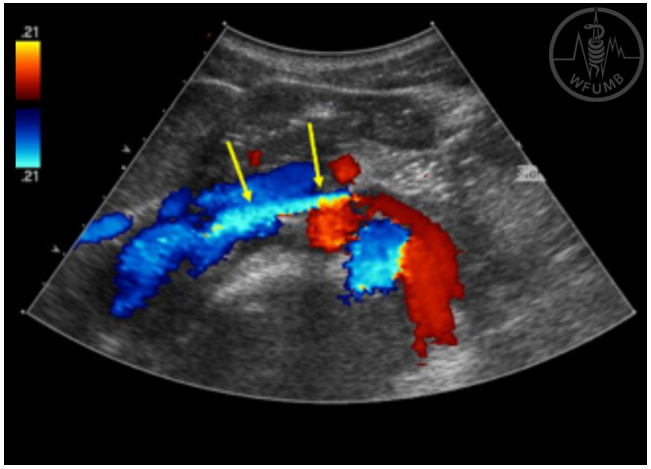

View enlarged image

Fig 17.12b
19-year-old man with gross hematuria caused by nutcracker syndrome. CDUS shows jetting of bright-colored high-velocity blood flow (arrows)

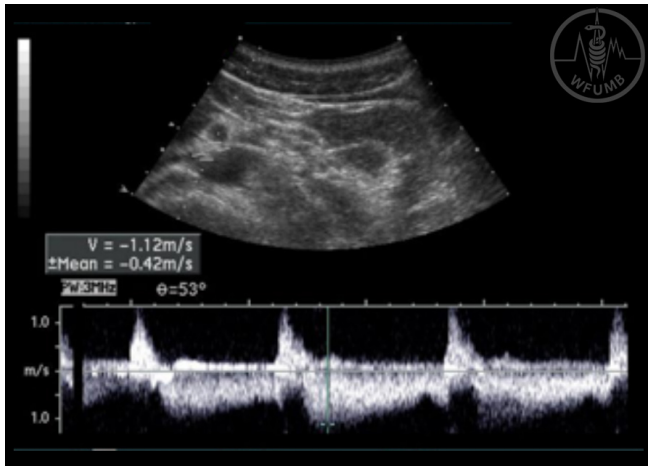

View enlarged image

Fig 17.12c
19-year-old man with gross hematuria caused by nutcracker syndrome. Peak flow velocity of LRV at aortomesenteric portion was 112 cm/sec

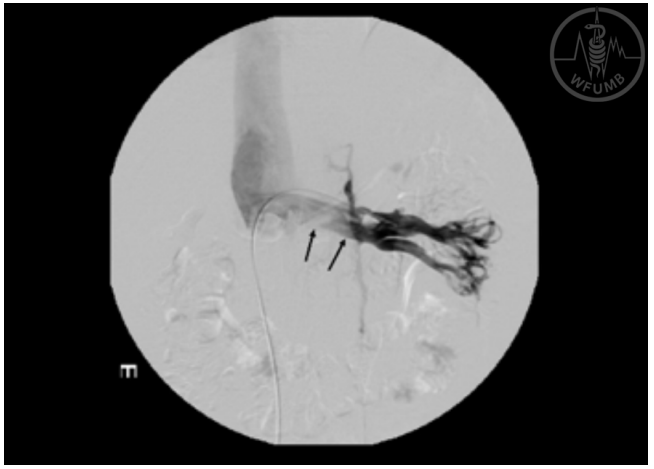

View enlarged image

Fig 17.12d
19-year-old man with gross hematuria caused by nutcracker syndrome. Left renal venography shows compression of LRV (arrows) and pressure gradient across the compressed aortomesenteric LRV was 4mmHg

17.1.9.3. Other renal vascular diseases

Renal Doppler US may demonstrate the lesions in other renal vascular disease such as aneurysm (Fig 17.13), arteriovenous fistula or malformation, renal infarction, or renal vein thrombosis. However, usually US imaging only is not enough and further evaluation with CT or MRI is needed.

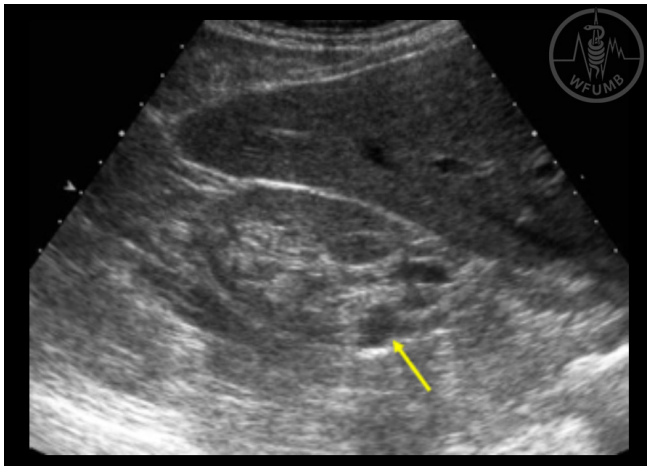

View enlarged image

Fig 17.13a
Calcified renal artery aneurysm in a 63-year-old man. Grey-scale US image of the right kidney shows a small round anechoic lesion (arrow) in the posterior aspect of the right kidney

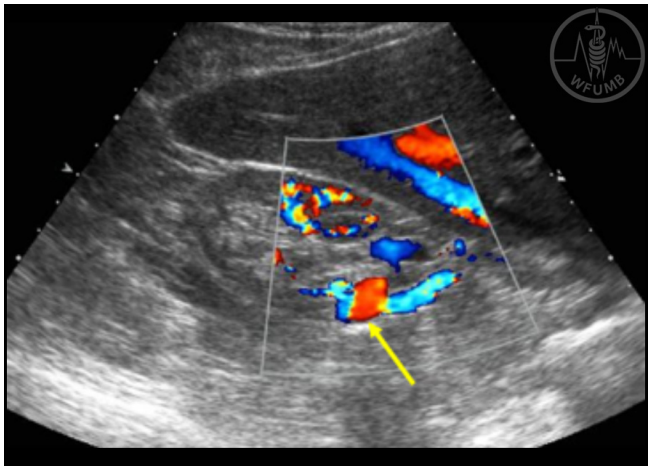

View enlarged image

Fig 17.13b
Calcified renal artery aneurysm in a 63-year-old man. CDUS shows that the lesion is filled with flow signals of various colors (arrows) indicating that the lesion is an aneurysm

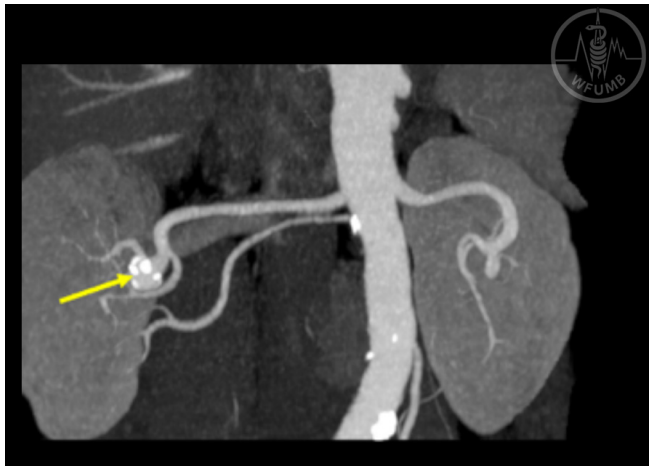

View enlarged image

Fig 17.13c
Calcified renal artery aneurysm in a 63-year-old man. CT angiography shows a calcified aneurysm in the right kidney

Remember

- In most renal parenchymal diseases, kidneys become smaller as disease progresses
- US alone is not enough to characterize solid renal masses and usually CT and/or MRI or CEUS are necessary for further evaluation
- US is helpful in detecting stones in the renal pelvicalyceal system and urinary bladder
- US, especially Doppler US, is a valuable tool in the evaluation renal artery stenosis

17.2. Ultrasound of the Adrenal Glands

17.2.1. Normal adrenal gland at ultrasound

Adrenal gland is an important endocrine gland but is too thin to be imaged properly with US. Adrenal masses, however, are often identified, and also the normal can be seen with most of the modern US machines, especially on the right side (Fig 17.14). Normal adrenal gland is composed of the cortex and medulla and the echogenicity of inner medulla is much higher than that of outer cortex.

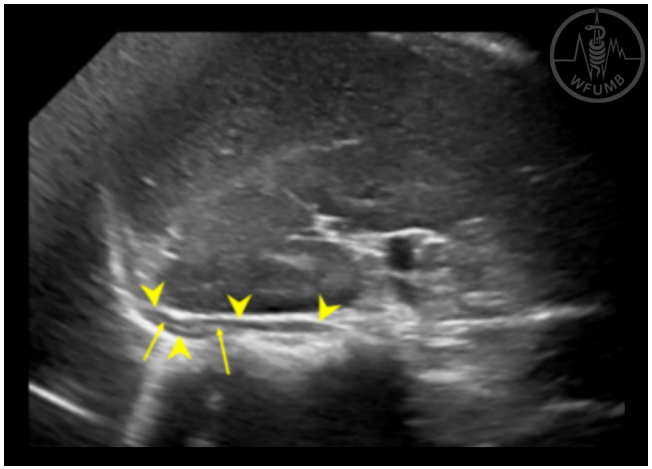

View enlarged image

Fig 17.14a
Normal US images of the adrenal gland in a 59-year-old woman. Longitudinal (US image of the right adrenal gland shows an elongated structure with hypoechoic peripheral cortex (arrowheads) and hyperechoic central medulla (arrows)

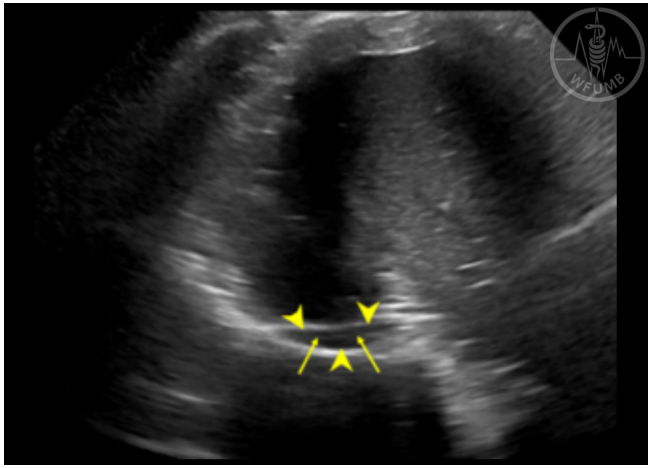

View enlarged image

Fig 17.14b
Normal US images of the adrenal gland in a 59-year-old woman. Transverse US image of the right adrenal gland shows an elongated structure with hypoechoic peripheral cortex (arrowheads) and hyperechoic central medulla (arrows)

17.2.3. Adrenal cysts

Adrenal cysts may be congenital, but more often they are formed from previous hemorrhage or trauma. Cysts can grow and cause pain especially when hemorrhage is associated. Calcification may be found on the cyst wall and infection may be complicated. US is excellent in distinguishing a cyst from a solid adrenal mass and follow up of an adrenal cyst.

17.2.4. Solid adrenal masses

The most common solid adrenal masses are adenomas but they are often too small to be evaluated with US. Other solid adrenal masses include pheochromocytoma, carcinoma, lymphoma, and metastasis. Characterization and differentiation of those solid adrenal masses with US is difficult. Adrenal myelolipoma, a benign adrenal tumor composed of fatty and bone marrow tissues, appears strongly hyperechoic, and may be diagnosed accurately with US (Fig 17.15).

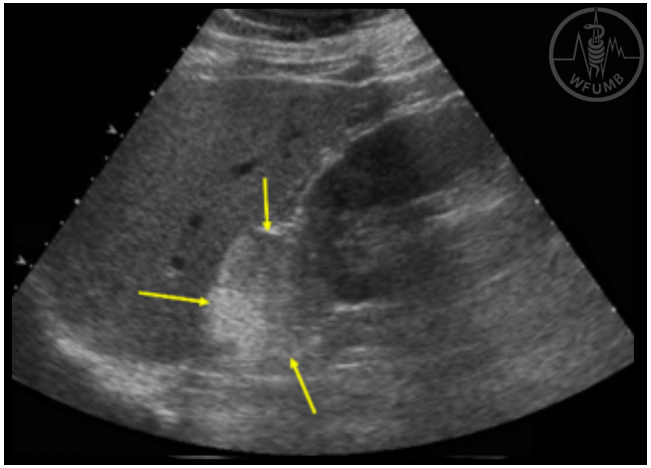

View enlarged image

Fig 17.15a
Adrenal myelolipoma in a 41-year-old man. Longitudinal US image of the right kidney shows a round mass of heterogeneous hyperechogenicity (arrows)

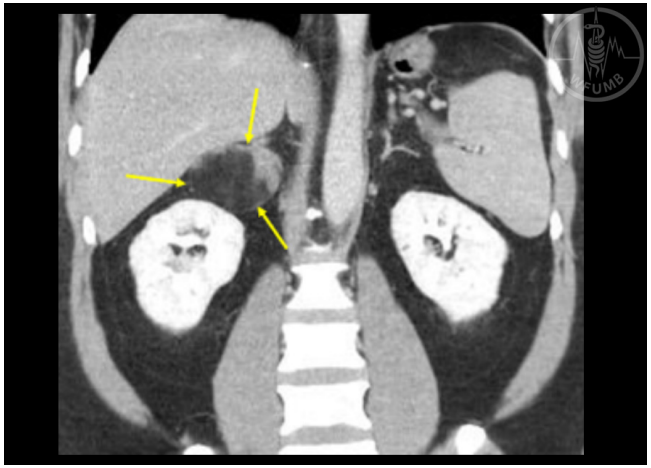

View enlarged image

Fig 17.15b
Adrenal myelolipoma in a 41-year-old man. Contrast-enhanced CT in coronal plane shows a right adrenal mass with fatty and non-fatty components (arrows)

Remember

- The most common solid adrenal masses are adenomas
- Characterization and differentiation of solid adrenal masses with US is difficult, with the exception of adrenal myelolipoma (benign adrenal tumor), which appears as strongly hyperechoic

17.3 CEUS in renal imaging

During last decade, contrast-enhanced ultrasonography (CEUS) has been successfully applied in renal imaging. This method overcomes many of the limitations of Doppler modes in evaluation of the vascularity of the kidney and of the renal lesions, and is able to replace contrast-CT and contrast-MRI in many cases in which such techniques were formerly necessary (→ Chapter 32).

17.3.1 Study procedure

After a preliminary grey-scale and color Doppler evaluation, the ultrasound equipment is set for contrast examination. A low mechanical index (MI) is used. After microbubble injection kidneys enhance rapidly and intensively. Signal is independent from the angle of insonation. The renal artery and the main branches enhance first, followed rapidly by the segmental, interlobar, arcuate and interlobular arteries and then complete cortical enhancement. Medullary enhancement follows, with the outer medulla enhancing first, followed by gradual fill-in of the pyramids. Contrary to enhancement observed after iodine- and gadolinium-based contrast agents there is no excretory phase.

17.3.2 Renal Ischemia

CEUS has an excellent diagnostic performance in the detection of renal parenchymal ischemia, similar to that of contrast-CT and contrast-MRI, also in patients with renal function impairment. This is particularly useful in patients with rapid deterioration of renal function in whom an ischemic cause for AKI is suspected clinically. Infarcts appear as wedge-shaped non-enhancing areas within an otherwise enhancing kidney.

17.3.3 Differentiation between solid and cystic renal lesions

Thanks to the high sensitivity to detect minimum blood flow, CEUS is highly effective to differentiate tumors from complex cysts presenting with echogenic or mixed sonographic appearance. Virtually all solid hypovascular tumors enhance at CEUS, while lesions without enhancement are characterized as benign cysts. This situation is relatively common, especially in patients with end-stage renal disease in whom an increased incidence of complex benign cysts and tumors is observed.

17.3.4 Differential diagnosis between solid renal masses and pseudotumors

CEUS is used to differentiate between renal tumors and mimicking anatomical variations not characterized with grey-scale imaging and conventional Doppler US. Pseudotumors have the same enhancing characteristics as the surrounding parenchyma in all phases, that means a pseudolesion not only displays isoenhancement to the parenchyma in both vascular phases but shows exactly the same enhancement pattern as the normal renal parenchyma: timing of enhancement and vascular architecture. In particular, a medullary portion and normal parenchymal vessel branching can be recognized in up to 70% and 45% of pseudotumours with equivocal appearance on conventional Doppler modes, respectively.

17.3.5 Characterization of complex cystic renal masses

CEUS is appropriate in the Bosniak classification of renal cysts, provided that the specific characteristics of US modes, compared to contrast-CT and contrast-MRI, are taken into consideration. The presence of calcifications hampers CEUS evaluation of complex cysts masses. If the lesion is well seen at US, however, CEUS is superior to contrast-CT to identify subtle enhancement, septa, and solid components. CEUS allows the characterization of renal cystic lesions as benign or malignant with at least the same accuracy as CT imaging, but contrast-CT remains the reference method for staging. CEUS is well suited for the follow- up of non-surgical complex cystic lesions and has potential to replace CT for this task. The absence of ionizing radiation is advantageous, as follow-up should prolong for several years.

17.3.6 Renal infections

The diagnosis of acute uncomplicated pyelonephritis is based on clinical examination and laboratory findings. Conventional B-mode US is used to exclude urinary obstruction and renal calculi. Additional investigations are considered in complicated pyelonethritis, especially if the patient remains febrile during the treatment. In these patients with complicated pyelonephritis, CEUS is effective in identifying abscesses, presenting as non-enhancing area, and areas of inflammatory involvement, which are relatively hypovascular, round or wedge-shaped, most conspicuous during the parenchymal late phase. CEUS can be used to monitor the resolution of abscesses, which can be delayed, also in patients with clinical improvement.

17.3.7 Renal traumas

CEUS allows a significant improvement in the diagnostic performance of the ultrasound imaging also in renal traumas. Renal injuries are seen as enhancement defects in the context of the healthy surrounding parenchyma. As a consequence, in patients with renal traumas CEUS is well suited for the follow-up, of the renal lesions not involving the urinary tract (→ Chapter 32).

The main indications of CEUS in kidney pathology are:

- Detection of renal parenchymal ischemia
- Characterization of tumors and pseudotumors
- Characterization and follow-up of complex cystic renal masses
- Diagnosis and follow-up of renal abscesses
- Diagnosis and follow-up of kidney lesions following trauma

Recommended reading

- Bertolotto M, Bucci S, Valentino M, Currò F, Sachs C, Cova MA. Contrast-enhanced ultrasound for characterizing renal masses. Eur J Radiol. 2018;105:41-48.
- Bertolotto M, Campo I, Sachs C et al. Contrast-enhanced ultrasound after successful cryoablation of benign and malignant renal tumours: how long does tumour enhancement persist. J Med Imaging Radiat Oncol. 2021
- Bertolotto M, Cicero C, Catalano O, Currò F, Derchi LE. Solid Renal Tumors Isoenhancing to Kidneys on Contrast-Enhanced Sonography: Differentiation From Pseudomasses. J Ultrasound Med. 2018;37:233-242.
- Bertolotto M, Siracusano S, Cicero C et al. Cryotherapy of Renal Lesions: Enhancement on Contrast-Enhanced Sonography on Postoperative Day 1 Does Not Imply Viable Tissue Persistence. J Ultrasound Med. 2017;36:301-310.
- Cantisani V, Bertolotto M, Clevert DA et al. EFSUMB 2020 Proposal for a Contrast-Enhanced Ultrasound-Adapted Bosniak Cyst Categorization - Position Statement. Ultraschall Med. 2020
- Girometti R, Stocca T, Serena E, Granata A, Bertolotto M. Impact of contrast-enhanced ultrasound in patients with renal function impairment. World J Radiol. 2017;9:10-16.
- Granata A, Bertolotto M. Imaging in Nephrology. Springer Nature, Switzerland AG; 2021
- Granata A, Zanoli L, Insalaco M et al. Contrast-enhanced ultrasound (CEUS) in nephrology: Has the time come for its widespread use. Clin Exp Nephrol. 2015;19:606-615.
- Martino P, Galosi AB. Atlas of Ultrasonography in Urology, Andrology, and Nephrology. Springer Nature, Switzerland AG; 2017.
- Sidhu PS, Cantisani V, Dietrich CF et al. The EFSUMB Guidelines and Recommendations for the Clinical Practice of Contrast-Enhanced Ultrasound (CEUS) in Non-Hepatic Applications: Update 2017 (Long Version). Ultraschall Med. 2018;39:e2-e44.

17.4. Videos


View enlarged video


View enlarged video


View enlarged video


View enlarged video


View enlarged video


View enlarged video